Impact of climate change on weather-related fire risk factors in the TWWHA Interim Report

Peter T. Love* Paul Fox-Hughes† Rebecca Harris*
Tom Remenyi* Nathan Bindoff*

August 24, 2016

Summary

Weather-related fire risk factors for the Tasmanian Wilderness World Heritage Area under a high emissions scenario in the Climate Futures for Tasmania downscaled climate models have the following broad characteristic projections:

- Decreasing frequency and extent (but not necessarily intensity) of widespread lightning outbreaks.
- Average conditions are projected to be less conducive to lightning.
- Indicators of fire danger relevant to dry eucalypt forest increase significantly with respect to both average conditions and the intensity of extreme events.
- Increasing mean fire danger in areas of buttongrass moorlands.
- Increases in fire danger indicators accelerate in the second half of the century.
- The most extreme values of buttongrass moorlands fire danger are projected to remain steady through to the end of the century.

*Antarctic Climate and Ecosystems Cooperative Research Centre
†Bureau of Meteorology, Hobart

Contents

1 TWWHA Future Lightning Potential derived from CFT data

The TWWHA area was examined to identify projected future dry lightning trends. Fields of "Lightning Potential Environment" (LPE) were calculated from the Climate Futures for Tasmania (CFT) model using the approach of *Rorig and Ferguson* [1999], together with the use of modest upward vertical motion (as operationally implemented in the Australian Bureau of Meteorology National Thunderstorm Forecast Guidance System, [*Deslandes et al.*, 2008]). A suitable 850–500 hPa temperature difference (in excess of 28 °C), difference between 850 hPa drybulb and dewpoint temperatures (in excess of 10 °C and upward vertical motion (in excess of 10 hPa/hr) identified pixels conducive to the occurrence of thunderstorms (areas identified as either '1' - suitable dry lightning environments - or '0', if unsuitable for the development of lightning).

For each day within the CFT dataset, four times were available for the calculation of the LPE: 0600, 1200, 1800 and 2400. Annual average values of the daily count of LPE were calculated for each time, as were the corresponding 99th percentile LPE count. Thus, for example, if 2020 has an annual average LPE value of 3 at 1800 hrs, that indicates that on average across the year, three grid cells within the TWWHA were conducive to dry lightning occurrence (i.e. had a value of 1) at 1800 each day. To smooth interannual variability, a 30-year running mean of these values was calculated. These values were calculated for each of the six models available within CFT, and a multi-model mean was also derived. The individual model values (colour) and multi-model mean 30-year running mean are displayed in Figure 1.

This suggests a decline in the average LPE across all models with time. Of course, average conditions do not represent the conditions under which lightning outbreaks occur (although they are useful, setting the background against which such outbreaks may occur, and suggesting that the latter will be more - or in this case - less likely to occur). Thus, 99th percentile values

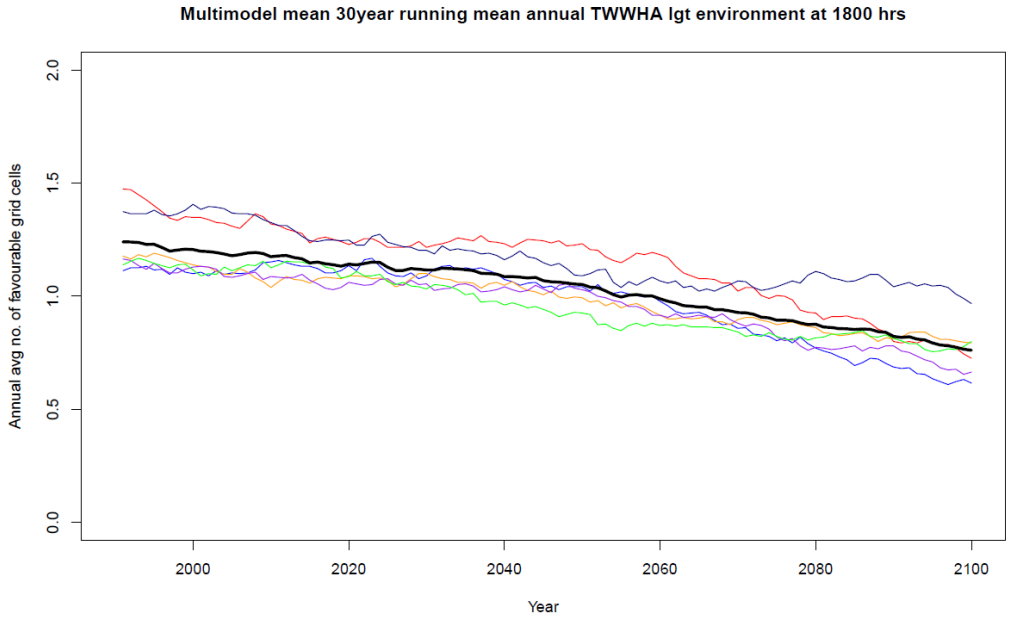

Figure 1: 30-year running mean of annual average LPE over the TWWHA. Coloured lines indicate individual CFT model values, the heavier black line shows the multi-model mean.

of annual average LPE over the TWWHA were also calculated i.e. the 99th percentile values of LPE over each year within the CFT dataset, again with interannual variability smoothed by calculating a 30-year running mean.

Again, a gradual decline through time is evident, although with greater variability than was the case for the average (Figure 2). This is consistent with the work of *Dowdy and Mills* [2012], where instability is projected to decrease with time, over the Australian region during the current century. This does not mean there will be no storms, or indeed a decline in activity levels of storms - it could be that storms may become more intense, just slightly less frequent. This may be possible to establish from a closer examination of the data. In addition, it will be valuable to compare these changes to those in soil moisture. The Future Fire Danger Technical Report from CFT [*Fox-Hughes et al.*, 2015] projected increased summer soil dryness in the western forecast district (which overlaps somewhat with the TWWHA) with time. It remains to identify whether there is a change in one particular variable that is driving the change in LPE.

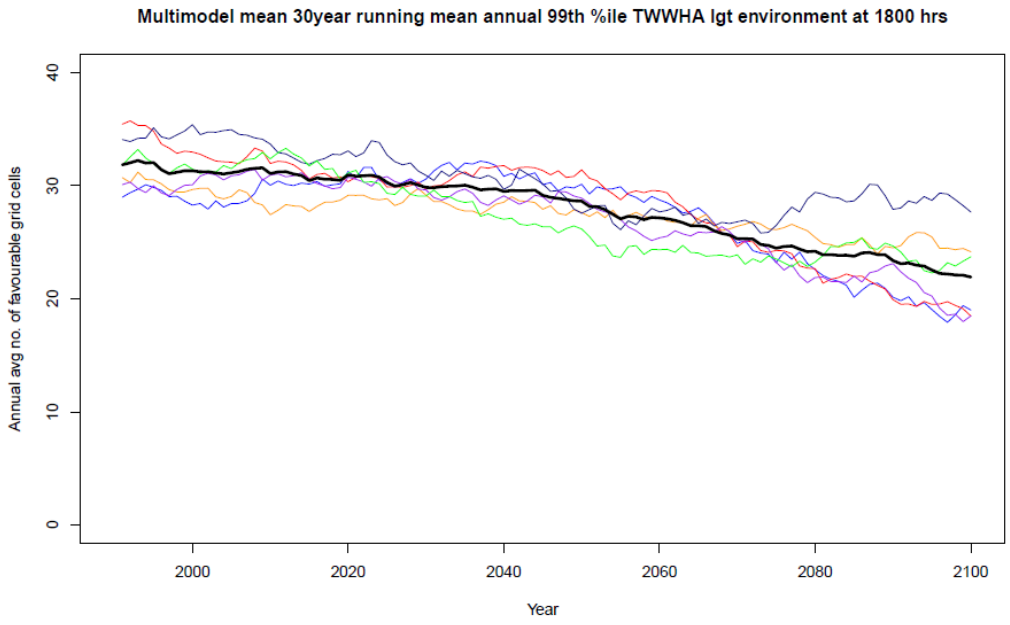

Figure 2: 30-year running mean of annual average 99th percentile LPE over the TWWHA. Coloured lines indicate individual CFT model values, the heavier black line shows the multi-model mean.

2 Projected Changes to Fire Danger Indices in the TWWHA and Influential Adjacent Reserves and Vegetation Westward of the TWWHA

2.1 McArthur Forest Fire Danger Index

The CFT Future Fire Danger project [*Fox-Hughes et al.*, 2015] produced statewide daily estimates of the McArthur Forest Fire Danger Index (FFDI) [*McArthur*, 1967; *Noble et al.*, 1980] from the output of each of the six CFT downscaled climate models for the period of 1961–2100 [*Corney et al.*, 2010]. The statistics of these FFDI data have been analysed here in a similar manner to that described in *Fox-Hughes et al.* [2014] for the regions of the Tasmanian Wilderness World Heritage Area (TWWHA) and the influential adjacent reserves and vegetation westward of the TWWHA (hereafter Adjacent Areas).

For each grid cell within the two regions of interest the 80th, 90th and 99th percentile, and mean FFDI values were calculated for each year of the CFT period and for each of the six models. These statistics were calculated for both the bushfire season (October–March) and for the full year (July–

June). Multi-model means of these statistics were then calculated for each grid cell. Mean values of each statistic were then calculated across the two regions.

The multi-model mean annual statistics for the TWWHA region are plotted in the left column of Figure 3 (black crosses) together with a 30-year running mean (black line). The 30-year running means for each individual model are also plotted in colour to indicate the inter-model variability. While the annual values exhibit large interannual variability, there is a clear increasing trend in each of the four statistics. The results are shown for the bushfire season only as the trends and variability in the full year statistics are very similar, the only notable difference being that the full year statistics are consistently lower than those for the fire season. The running means show significant internal variability within the models on decadal time-scales, however the increasing trend is consistent and accelerates towards the end of the period. These results are consistent with the analysis of the Western region of *Fox-Hughes et al.* [2014]. The same statistics for the Adjacent Areas region, plotted in the right column of Figure 3, are consistently lower than the TWWHA but otherwise share very similar characteristics.

The same statistics were also calculated across four 20-year periods, baseline (1980-2000), near-future (2010-2030), mid-century (2040-2060) and late century (2080-2100). This analysis is summarised for the bushfire season in Table 1. Values in parentheses are the percentage increase over the baseline period. The largest absolute increase is in the 99th percentile while the largest percentage increase is in the 80th percentile. The percentage increases are considerably higher in the Adjacent Areas. A large increase in the mean FFDI indicates that conditions in general will be more conducive to fire across both regions, while the increases in the percentile values indicate that the fire danger on high risk days will become more intense. The increase in the 99th percentile is smaller than the other percentiles but is still significant, indicating that the fire risk on the two days of most extreme fire danger during the fire season will be significantly higher by the end of the century, and indicates that the number of days with fire risk above the value of the 99th percentile during the baseline period will likely increase throughout the century.

A summary of the same statistics calculated over full years is presented in Table 2. While FFDI values are consistently lower over the full year, the characteristics are generally very similar to those of Table 1, although here the largest percentage increase is in the 90th percentile for both regions.

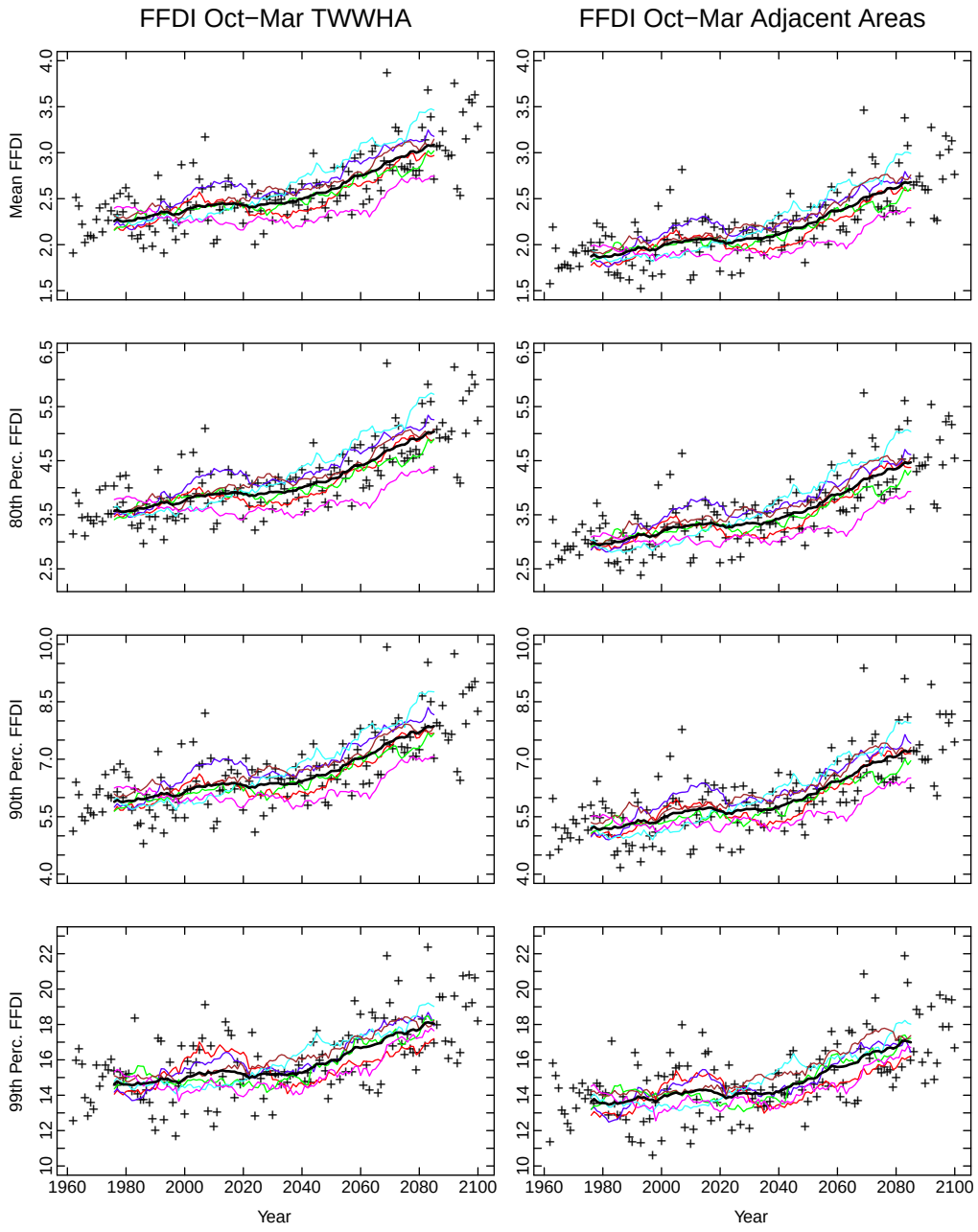

Figure 3: Projected forest fire danger index statistics for the TWWHA (left) and the influential adjacent reserves and vegetation westward of the TWWHA (right). Regional mean of yearly mean and percentile multi-model mean statistics (crosses), 30-year running mean (black line) and 30-year running means of individual models (colour lines).

October–March FFDI				
Period	Mean	80th Perc.	90th Perc.	99th Perc.
TWWHA				
1980–2000	2.24	3.49	5.85	16.54
2010–2030	2.49 (7.0)	3.76 (7.8)	6.28 (7.5)	17.51 (5.9)
2040–2060	2.60(16.0)	4.09 (17.2)	6.71 (14.8)	18.54(12.1)
2080–2100	3.19(42.3)	5.20 (48.9)	8.30 (41.9)	20.92(26.5)
Adjacent Areas				
1980–2000	1.84	2.86	5.11	15.22
2010–2030	2.01 (8.9)	3.16 (10.5)	5.61 (9.9)	16.29 (7.0)
2040–2060	2.22(20.5)	3.53 (23.7)	6.07 (18.9)	17.30(13.6)
2080–2100	2.77(50.5)	4.61 (61.4)	7.63 (49.4)	19.87(30.5)

Table 1: McArthur Forest Fire Danger Index statistics summary for TWWHA and Adjacent Areas during bushfire season. Values in parentheses are percentage increases over the baseline period (1980–2000).

Full year FFDI				
Period	Mean	80th Perc.	90th Perc.	99th Perc.
TWWHA				
1980–2000	1.36	1.88	3.66	13.10
2010–2030	1.44 (5.9)	1.98 (5.0)	3.91 (6.8)	13.98 (6.7)
2040–2060	1.54(13.0)	2.15 (14.5)	4.19 (14.3)	14.43(10.1)
2080–2100	1.86(36.2)	2.15 (41.5)	5.27 (44.0)	16.75(27.8)
Adjacent Areas				
1980–2000	1.07	1.36	3.00	11.97
2010–2030	1.15 (7.4)	1.44 (5.4)	3.28 (9.1)	12.95 (8.2)
2040–2060	1.25(16.5)	1.62 (18.9)	3.60 (19.7)	13.54(13.1)
2080–2100	1.55(43.7)	2.08 (52.7)	4.67 (55.2)	15.86(32.5)

Table 2: As for table 2 but calculated over full years.

2.2 Buttongrass Moorland Fire Danger Index

Daily values of the Moorland Fire Danger Index (MFDI) [*Marsden-Smedley et al.*, 1999] were calculated from the output of the six CFT downscaled climate models for the full CFT period. The statistics of these MFDI data were then calculated as for the FFDI in the previous section.

Annual mean, 80th, 90th and 99th percentile MFDI for the TWWHA and Adjacent Areas regions are plotted in Figure 4 as for FFDI in Figure 2. Mean MFDI is projected to increase through the century in both regions, subject to considerable interannual and interdecadal variability. The 80th

percentile exhibits a similar increase, while the trend in the 90th percentile is less pronounced. A slight decrease in the 99th percentile is evident, although the uncertainty in this trend encompasses potential increases too. Similar to the FFDI, the MFDI for the Adjacent Areas are consistently lower than for the TWWHA while the characteristic trends and variability are very similar. Again, the results for the full year calculations exhibit consistently smaller values but have very similar trends and variability.

Statistical summaries of MFDI across the same four 20-year periods as for FFDI in Tables 1 and 2 are presented in Tables 3 and 4. The percentage increase in these statistics is low compared to the FFDI and in some cases negative, although the confidence in some of the smaller percentages is low. The largest percentage increases are seen in the mean and 80th percentile. The percentage changes are slightly larger in the Adjacent Areas than the TWWHA.

October–March MFDI				
Period	Mean	80th Perc.	90th Perc.	99th Perc.
TWWHA				
1980–2000	3.68	5.81	8.05	15.02
2010–2030	3.86 (0.0)	5.82 (0.0)	8.04 (-0.1)	14.77(-1.5)
2040–2060	3.73 (1.4)	5.93 (2.0)	8.08 (0.3)	14.87(-1.0)
2080–2100	3.89 (5.7)	6.26 (7.6)	8.3 (3.2)	14.87(-1.0)
Adjacent Areas				
1980–2000	3.37	5.35	7.36	14.40
2010–2030	3.37(-0.2)	5.35 (-0.1)	7.36 (-0.0)	14.24(-1.1)
2040–2060	3.46 (2.4)	5.51 (3.1)	7.47 (1.5)	14.31(-0.7)
2080–2100	3.60 (6.5)	5.82 (8.8)	7.67 (4.2)	14.04(-2.5)

Table 3: Moorland Fire Danger Index statistics summary for TWWHA and Adjacent Areas during bushfire season. Values in parentheses are percentage increases over the baseline period (1980–2000).

In relation to the projected changes in the parameters underlying the MFDI calculations, determined by the CFT climate modelling [*Corney et al.*, 2010], the trend in the projected mean MFDI is consistent with increasing temperatures accelerating in the second half of the century. The MFDI is particularly sensitive to wind strength which is projected to decrease during fire season, potentially offsetting the effects of increases in temperature. This could account for the much smaller increase in MFDI than FFDI. Rainfall in western Tasmania is projected to decrease during summer in the second half of the century, while increasing during winter. Despite these changes there

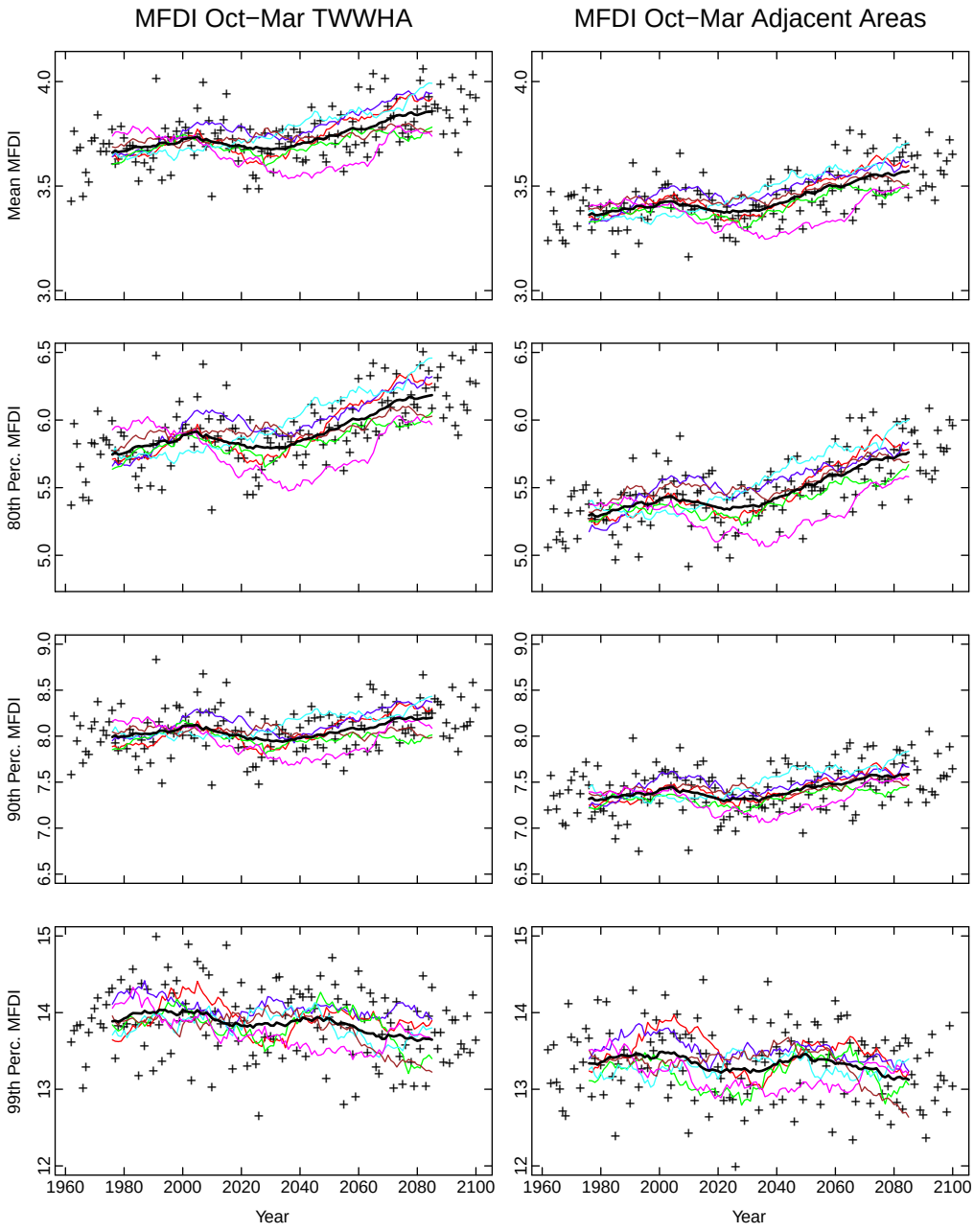

Figure 4: As for figure 2 but for Moorland Fire Danger Index.

is little difference between the trends in the fire season and full year MFDI statistics. However, MFDI is most sensitive to time since last rainfall so changes to the frequency of rainfall events need to be assessed to understand how rainfall is driving changes to MFDI. An assessment of the changes to the extreme values of these parameters will be necessary to understand the changes, or apparent lack thereof, to the occurrence of days of extreme MFDI.

	Full year MFDI			
Period	Mean	80th Perc.	90th Perc.	99th Perc.
TWWHA				
1980–2000	3.33	4.9	7.41	14.12
2010–2030	3.36(0.8)	4.94 (1.0)	7.43 (0.2)	14.03(-0.6)
2040–2060	3.42(2.5)	5.07 (3.6)	7.50 (1.2)	14.15 (0.2)
2080–2100	3.56(6.7)	5.37 (9.7)	7.74 (4.4)	14.27 (1.1)
Adjacent Areas				
1980–2000	2.96	4.25	6.52	13.23
2010–2030	2.97(0.2)	4.27 (0.5)	6.50 (-0.2)	13.15(-0.6)
2040–2060	3.03(2.3)	4.43 (4.2)	6.60 (1.2)	13.21(-0.1)
2080–2100	3.14(6.0)	4.69 (10.5)	6.80 (4.3)	13.18(-0.3)

Table 4: As for table 3 but calculated over full years.

References

Corney, S. P., J. J. Katzfey, J. L. McGregor, M. R. Grose, J. C. Bennett, C. J. White, G. K. Holz, S. M. Gaynor, and N. L. Bindoff (2010), Climate Futures for Tasmania: climate modelling technical report, *Tech. rep.*, Antarctic Climate and Ecosystems Cooperative Research Centre, Hobart Tasmania.

Deslandes, R., H. Richter, and T. Bannister (2008), The end-to-end severe thunderstorm forecasting system in Australia: overview and training issues, *Aust. Meteorol. Mag*, *57*(4), 329–343.

Dowdy, A., and G. A. Mills (2012), Atmospheric and fuel moisture characteristics associated with lightning-attributed fires, *J. Appl. Meteorol. Clim.*, *51*(11), 2025–2037, doi:10.1175/JAMC-D-11-0219.1.

Fox-Hughes, P., R. M. B. Harris, L. G., G. M., and N. L. Bindoff (2014), Future fire danger climatology for Tasmania, Australia, using a dynamically downscaled regional climate model, *Int. J. Wildland Fire*, *23*(3), 309–321, doi:10.1071/WF13126.

Fox-Hughes, P., R. M. B. Harris, L. G., J. Jabour, G. M., T. A. Remenyi, and N. L. Bindoff (2015), Climate Futures for Tasmania future fire danger: the summary and the technical report, *Tech. rep.*, Antarctic Climate and Ecosystems Cooperative Research Centre, Hobart, Tasmania.

Marsden-Smedley, J. B., T. Rudman, A. Pyrke, and W. R. Catchpole (1999), Buttongrass moorland fire-behaviour prediction and management, *Tas-forests*, *11*, 87–107.

McArthur, A. G. (1967), *Fire behaviour in eucalypt forests*, Forestry and Timber Bureau, Canberra.

Noble, I. R., A. M. Gill, and G. A. V. Bary (1980), McArthur's fire-danger meters expressed as equations, *Aust. J. Ecol.*, *5*(2), 201–203, doi: 10.1111/j.1442-9993.1980.tb01243.x.

Rorig, M. L., and S. A. Ferguson (1999), Characteristics of lightning and wildland fire ignition in the Pacific Northwest, *J. Appl. Meteorol.*, *38*(11), 1565–1575, doi:10.1175/1520-0450(1999)038<1565:COLAWF>2.0.CO;2.